

Received: 12 January 2024 / Accepted: 25 February 2024 / Published online: 08 March 2024

*thermovision, thermography,
machining by turning,
cutting zone*

Andrzej UHRYNSKI¹, Saltanat NURKUSHEVA^{2,3},
Muratbek USSERBAYEV⁴, Pawel HYL⁵,
Michał BEMBENEK^{5*}

A COMPARATIVE THERMAL ANALYSIS OF TWO WORKPIECE MATERIALS OF DIFFERENT MACHINABILITY WHEN TURNING BASED ON IR THERMOGRAPHY

The comparative thermography analysis of temperature during machining by turning was presented. For the tests cast iron EN-GJL 250 and stainless steel 1.4301 were used. The machining by turning was performed with the TNMG 220408HS PC9030 and TNMA 220208 NC6210 cutting inserts design for machining that kind of materials. The temperature was measured on the machined material and on the surface of the cutting insert. The temperature distribution was performed during 3 subsequent turning passes; therefore, the coolant was not used during machining. The emissivity of TNMG 220408HS PC9030 and TNMA 220208 NC6210 cutting inserts was performed. In the case of EN-GJL-250 cast iron, the tests have shown that due to safety reasons (the lack of the safety cover in the working area of the lathe) it was impossible to perform the measurements at the highest assumed machining speed of 339.1 m/min. The higher average temperatures in the material were recorded for 1.4301 steel, even though the machining process was performed at a much lower machining speed than in the case of EN-GJL-250 cast iron. The average cutting insert temperature when turning EN-GJL-250 cast iron was approximately 100°C higher than for 1.4301 steel.

1. INTRODUCTION

The thermal imaging process was discovered in the 19th century [1], but it came into common use in the 21st century, thanks to widely available thermal imaging cameras [2]. The current use of the thermal imaging process is not limited only to obvious applications, such as building insulation measurements [3, 4], or brake pad temperature [5], but it is

¹ Department of Machine Design and Maintenance, AGH University of Krakow, Poland

² Department of Transport Equipment and Technologies, S. Seifullin Kazakh Agro Technical Research University, Kazakhstan

³ Department of Organization of Transport, Traffic and Transport Operations, L.N. Gumilyov Eurasian National University, Kazakhstan

⁴ Department of Technological Machines and Equipment, S. Seifullin Kazakh Agro Technical Research University, Kazakhstan

⁵ Department of Manufacturing Systems, AGH University of Krakow, Poland

* E-mail: bembenek@agh.edu.pl

<https://doi.org/10.36897/jme/185359>

increasingly being used in less obvious scientific research, such as ice migration [6], or fine-grained materials transport monitoring [7]. Recent literature reports also indicate that thermal imaging can also be used to measure humidity [8] or in the process of detecting breast cancer [9]. Using thermography may apply not only to static conditions but also to optimization [10], diagnostics [11–13], as well as monitoring [14] of the technological process.

The proper selection of machining parameters is crucial for the dimensional accuracy of the workpiece [15–17], the quality of the machined surface [18–20], production time [21] and manufacturing costs [22, 23]. One of the main problems in the machining by turning, from the technological point of view is the fact some part of the energy consumed on the turning process is converted to heat [24–26] and it must be properly transmitted out of the processing zone [27]. Usually, a high temperature in the cutting zone depends on many factors e.g. material, toll, tool cover [28] and what is not desirable can change the microstructure of the steel [29, 30] and the surface layer hardness [31]. This effect can be reduced, e.g. by using coolants [32, 33].

Temperature changes in the turning zone influence on the process e.g. increasing the machining resistance and power consumption [34, 35] and can cause a negative impact on machinability difficulties in chip breaking and tool wear. Modern measuring techniques still provide many problems in the monitoring of machining parameters in real-time [36]. Therefore, thermal imaging is increasingly used for these type of measurements. In the literature, thermographic studies can be found, among others: machining of specific materials such as stainless steel [37], temperature measurement taking into account material consumption [38] and radial turning in specific conditions [27, 39]. However, there is a lack of comparative studies analyzing the temperature distribution of the cutting insert and the machining material while turning steel and cast iron.

This article presents the research on the temperature distribution in the turning zone of two different materials: cast iron EN-GJL250 and stainless steel 1.4301. The temperature distribution was measure during three subsequent machining passes; therefore the coolant was not used during machining, not to influence on accuracy of the research. Before the tests, the emissivity of carbide cutting inserts for turning both materials was performed.

2. MATERIAL AND METHODS

2.1. MATERIALS

To perform the thermography test of machining by turning of two different materials EN-GJL-250 cast iron and 1.4301 stainless steel were used. The chemical compositions of both materials with selected mechanical properties are presented in Table 1. EN-GJL-250 is a grey cast iron with flake graphite. It is characterized by good thermal conductivity, good machinability and vibration damping. Its structure does not change in the temperatures up to 600°C so it can be used in an environment with quite high temperature [37, 39].

Whereas 1.4301 stainless steel is one of the most popular acid-resistant steels. It is characterized by high susceptibility to plastic processing and welding. It has a wide range

of applications from food to the chemical industry [41]. Two shafts with a diameter of 40 mm of 1.4301 steel and 60 mm of EN-GJL-250 cast iron were used for the tests. The difference in diameters results from the facts of limited rotation speed of the lathe spindle and applying the corrected machining speeds suggested by manufacturer of the cutting insert.

Table 1. Chemical composition and selected mechanical properties of materials used in tests [40, 41]

Chemical element	EN-GJL-250	1.4301	Mechanical parameters	EN-GJL-250	1.4301
	Content, %			Value	
C	3.38	≤0.07	Maximum tensile stress R_m , MPa	250-350	500-700
Si	2.26	≤0.80			
Mn	0.52	≤2.0			
P	0.08	0.045			
S	0.06	0.03	Brinell hardness, HB	180-220	215
Cr	-	17.0-19.0			
Ni	-	9.00-11.00	Fracture toughness k_c , MPa	1000	2000

2.2. THE TURNING PROCESS

Cutting inserts manufactured by Korloy (Korloy, Seoul, Republic of Korea) selected for turning steel and cast iron were used for machining tests. The cutting inserts were brand new, and the purpose of this article was not to take into account the change in machining by turning as they wore. The parameters of inserts are presented in Table 2. Turning tests were carried out on the universal lathe TUD 50 (WAFUM, Wroclaw, Poland). The turned shafts were mounted in a three-jaw chuck.

Table 2. Machining parameters of cutting inserts.

Cutting inserts type / Material	Type of turning material	Machining speed [m/min.]	Machining depth [mm]	Feed rate [mm/rev.]	Coating
TNMG 220408HS PC9030	Stainless steel	50–80	1.0-4.0	0.1–0.4	TiAlN
TNMA 220208 NC6210	Cast iron	250–450	1.0–6.0	0.15–0.6	Al ₂ O ₃ MT–TiCN

The machining parameters were selected depending on the type of machined material and they were different within the range specified by the manufacturer of the cutting inserts and literature recommendation [42, 43]. The machining speed was ultimately determined by the lathe's gear ratio. Detailed informations of the machining parameters are provided in Table 3. The machining depth for all tests was 1 mm. The machining parameters were calculated based on [43]. Three series of tests were carried out for each roller. For the nominal diameter of the shaft, for the diameter after the first turning 2 mm smaller than the nominal diameter and for the diameter after the second turning 4 mm smaller than the nominal diameter.

Table 3. The machining parameters of the test.

Material	Tool	D_m [mm]	v_c [m/min]	a_p [mm]	f_n [mm/rev.]	P_c (calculated) [kW]	n [rpm]
1.4301	TNMG 220408HS PC9030	40	113.0	1	0.20	7.54	900
		38	84.7	1	0.20	5.65	710
		36	50.9	1	0.20	3.39	450
EN-GJL 250	TNMA 220208 NC6210	60	339.1	1	0.37	20.91	1800
		58	220.4	1	0.37	13.59	1210
		56	196.9	1	0.37	12.14	1120

2.3. CUTTING INSERTS EMISSIVITY PARAMETER EXAMINE

To determine the emissivity of the cutting inserts a special equipment presented in Fig. 1 was used.

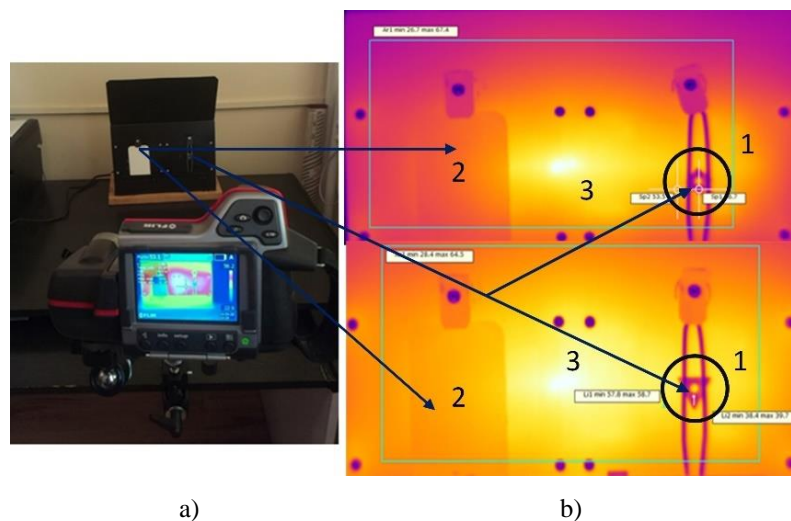


Fig. 1. Emissivity measurement scheme: a) the laboratory stand for determining the object's emissivity, b) the thermography images. 1 – cutting inserts, 2 – area with known emissivity value, 3 – heat source generator.

The measurements were done with the use of the FLIR T335 Thermal Imaging Camera (Wilsonville, Oregon, USA). To determine the emissivity of the cutting inserts, they were sequentially mounted on a measuring device. During the experiments, the air humidity was 40% and the ambient temperature was 24°C. The images were taken from 0.8 m. In the next step, boundary conditions related to air humidity, the distance between the camera lens and the object, and ambient and air temperatures were set up. Then, the temperature of the reference object with known emissivity was measured and the measuring point was moved to the cutting inserts. The emissivity was selected so that the temperature of the reference object and the cutting insert were the same. The final emissivity value was determined as the arithmetic mean of three independent measurements for each sample. The analysis of obtained thermograph images was done with FLIR QuickReport 1.2 SP1.

2.4. TEMPERATURE MEASUREMENT DURING MACHINING TURNING

The measurements during machining turning were done with the use of the FLIR T335 Thermal Imaging Camera (Wilsonville, Oregon, USA). The camera was properly prepared for testing, the following calibration parameters were introduced: ambient temperature, reflection temperature, relative humidity, distance from the tested object and emissivity of the material. Unnecessary sources of radiation were also eliminated and convection in the room was limited. Thermal images were taken from the distance of approximately 0.5 m from the cutting zone. For each pass, five images were taken at different places where the shafts were machined. The analysis of obtained thermograph images was done with FLIR QuickReport 1.2 SP1. By analyzing the thermographic images, the temperature in the cutting zone and the tool (cutting insert) temperature were determined. A view of the lathe with a mounted shaft and a sample of the thermographic image at the ambient temperature are shown in Fig. 2.



Fig. 2. Thermal imaging laboratory stand: a) the cast iron shaft mounted in the TUD50 lathe, b) thermography image taken with FLIR 335 camera in room conditions temperature

The temperature of the cutting inserts during machining was determined on the bisector of the angle running from the cutting tip, approximately 5 mm from the machining zone (Fig. 3).

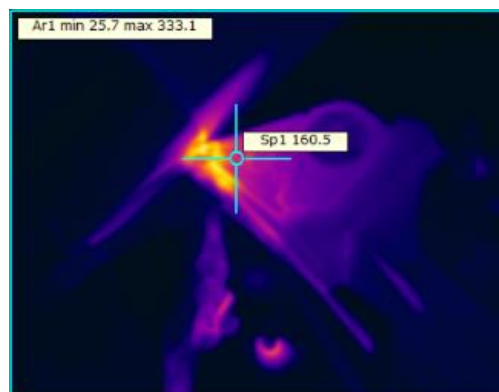


Fig. 3. The place of measuring the cutting insert temperatures during turning (turning of 1.4301 steel at machining speed 84.7 m/min. the 5th measurement)

3. RESULTS AND DISCUSSION

The results of the emissivity of the cutting inserts are presented in Table 4. The test results indicate that there is not much difference between the emissivity values of the cutting inserts. This is because both tested materials are black and matte, and the differences in the features affecting the emissivity value are small. The obtained emissivity results correspond to the emissivity values of steel and cast iron used for testing [44].

Table 4. The results of the emissivity of cutting inserts used in the experiment

Cutting inserts type / Material	Measurement			Estimated emissivity
	1	2	3	
TNMG 220408HS/PC9030	0.39	0.47	0.39	0.417±0.05
TNMA 220208/NC6120	0.38	0.37	0.36	0.372±0.01

The results of temperature measurements of the cutting inserts and the material are presented in Table 5 and Fig. 4. In the case of EN-GJL-250 cast iron, laboratory tests have shown that due to safety reasons, because of the lack of a cover in the working area of the lathe, it was impossible to carry out measurements at the highest assumed machining speed of 339.1 m/min. During the turning process at that speed, small chips were created, spreading at very high speed in all directions (Fig. 5). As it turned out during the research, the possible time of taking good quality thermoimages with the FLIR T335 Thermal Imaging Camera was equal to 5 seconds at a feed of 0.37 mm/rev. It only allowed for taking a limited number of images for the installed shaft length.

Table 5. The temperature measuring during the turning process

Material	Measuring point	V_c [m/min]	Temperature, °C				
			1	2	2	4	5
1.4301	cutting zone	113.0	360.1	338.2	331.5	359.8	360.3
		84.7	319.2	322.8	343.5	355.0	333.1
		50.9	348.2	310.0	358.2	318.2	330.6
	tool (cutting insert)	113.0	109.7	166.7	190.4	188.4	202.4
		84.7	129.7	113.8	143.0	155.9	160.5
		50.9	115.3	178.2	159.8	170.4	175.5
EN-GJL-250	cutting zone	339.1	-	-	-	-	-
		220.4	273.5	311.0	316.5	-	-
		196.9	288.7	329.0	324.7	329.3	320.3
	tool (cutting insert)	339.1	-	-	-	-	-
		220.4	186.9	212.8	240.5	-	-
		196.9	144.6	196.4	233.9	217.5	266.1

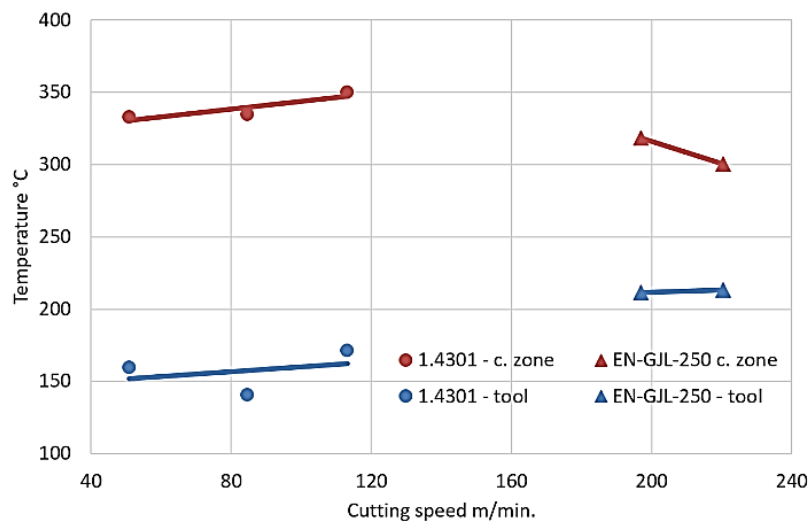


Fig. 4. The average temperature measuring of cutting inserts and machining materials during the turning process

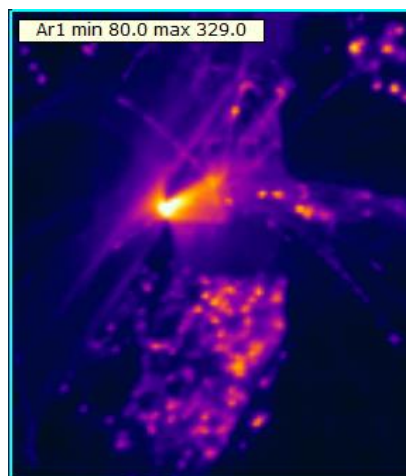


Fig. 5. The hot small chips created during turning of the EN-GJL-250 cast iron spreading in all directions (machining speed 196.9 m/min, the 2nd measurement) – the original picture without adjusting emissivity in the software

The range of measured temperatures in all tests was from 115.3°C to 360.3°C. Despite several times lower machining speed, the higher average temperatures in the cutting zone were recorded for 1.4301 steel. The average cutting insert temperature when turning EN-GJL-250 cast iron was approximately 100°C higher than for 1.4301 steel. Based on the results in Table 5, in the case of steel 1.4301 for machining speeds of 50.9 and 113.0 m/min the lower and the higher than the specific speed, respectively, the material temperature was higher at the beginning of machining, and then it decreases slightly and increases again. This can be explained by a sharp increase in machining resistance when the tool enters the material with inappropriate machining parameters [41]. A further increase in temperature can be explained by the natural processes of energy accumulation in the material and the greater absorption of energy than its release in convection processes to the environment. When machining with the recommended parameters, the material temperature in the cutting zone gradually

increases, which seems to be a natural process. Additionally, the first measurements could have been influenced by a change in surface emissivity. Covering the machined part of the shaft with an aerosol paint layer was considered. However, based on research [37], it can be assumed that this coverage has a very slight impact on the measurement results. When turning steel, temperatures determined at the cutting insert show a steady increase with machining progress. The interference occurring during measurements is most likely related to radiation from separating chips.

In the case of EN-GJL-250, it was impossible to carry out experiments at the highest machining speed for staff and equipment safety reasons. The ambiguity of the test results may be caused by the cloud of flying hot chips interfering with the camera reading. Analyzing the test results included in Table 5, one can notice a change in heat distribution depending on the machining speed. The temperature measurement in the cutting zone shows higher temperatures at lower machining speeds, while the tool temperature is higher at higher machining speeds. This may be due to the lower amount of heat dissipated from the material by chips when turning at a lower machining speed [41].

4. CONCLUSION

As research has shown, non-contact temperature measurement while machining by orthogonal turning without the use of coolant in the cutting zone using a thermal imaging camera is possible and seems to be interesting and developmental. The research performed does not exhaust the topic of the selected issue. Their purpose was only to check the possibility of using a thermal imaging camera to determine the temperature in the cutting zone. It was possible to precisely determine the emissivity of the used cutting inserts. This enables non-contact testing of the tool's operating temperature with high accuracy. The higher average temperatures in the cutting zone around 340°C were recorded for 1.4301 steel, even though the machining process took place at a much lower machining speed than in the case of EN-GJL-250 cast iron. The measurements show that increased machining temperature occurs both at machining parameters higher and lower than the range recommended by the manufacturer. During the machining process by turning, after a rapid increase in the temperature of both cutting insert at the beginning of machining, it was then possible to observe a slow increase in the temperature of both tools during their operation. The cutting insert when turning cast iron heated more than steel ones, which can be explained by the higher machining speed. The imaging frequency turned out to be an important factor for the experiment. The FLIR T335 camera were abler to take images every 5 seconds, which required the use of a large amount of processed material to obtain statistically significant results. The use of a higher frequency of taking images camera in the future would improve the research quality. The future tests will be carried out using a lathe with a higher engine power and a higher spindle speed range. The future tests need an additional equipment for the camera, such as a cover to protect the lens (and preferably the entire camera) against chips and a holder to mount the device to the machine tool support with the ability to adjust the viewing angle. The approximation of the experimental conditions to the real conditions occurring in the industry allows this method to be used in practice: when controlling the machining process or tool wear.

ACKNOWLEDGEMENTS

The authors would like to thank Mr. Adam Kuzniar for his participation in the laboratory test and for collecting the data which was used to prepare that article. The publication was financed by Subsidy grants number 16.16.130.942/KPiEM and 16.16.130.942/KSW

REFERENCES

- [1] MINKINA W., 2021, *How Infrared Radiation Was Discovered—Range of This Discovery and Detailed*, Appl. Sci., 11, 9824, <https://doi.org/10.3390/app11219824>.
- [2] SZAJEWSKA A., 2017, *Development of the Thermal Imaging Camera (TIC) Technology*, Procedia Engineering, 172, 2017, 1067–1072, <https://doi.org/10.1016/j.proeng.2017.02.164>.
- [3] KIM H., LAMICHHANE N., KIM C., SHRESTHA R., 2023, *Innovations in Building Diagnostics and Condition Monitoring: A Comprehensive Review of Infrared Thermography Applications*, Buildings, 13, 2829, <https://doi.org/10.3390/buildings13112829>.
- [4] TOMITA K., CHEW M.Y.L., 2022, *A Review of Infrared Thermography for Delamination Detection on Infrastructures and Buildings*, Sensors, 22, 423, <https://doi.org/10.3390/s22020423>.
- [5] BORAWSKI A., 2019, *Common Methods in Analysing the Tribological Properties of Brake Pads and Discs – a Review*, Acta Mechanica et Automatica, 13/3, 189–199.
- [6] YOUSUF A., KHAWAJA H., VIRK M.S., 2024, *A Review of Infrared Thermography Applications for ice detection and mitigation*, Cold Regions Science and Technology, 218, 10458.
- [7] KAMPCZYK A., GAMON W., GAWLAK K., 2022, *Implementation of Non-Contact Temperature Distribution Monitoring Solutions for Railway Vehicles in a Sustainability Development System Transport*, Sensors, 22, 9624, <https://doi.org/10.3390/s22249624>.
- [8] BUHCZIK D., BUDZAN S., KRAUZE O., WYZGOLIK R., 2023, *Moisture Determination for Fine-Sized Copper Ore by Computer Vision and Thermovision Methods*, Sensors, 23, 1220, <https://doi.org/10.3390/s23031220>.
- [9] OWENS A., KANDLIKAR S.G., PHATAK P., 2021, *Potential of Infrared Imaging for Breast Cancer Detection: A Critical Evaluation*, ASME J. of Medical Diagnostics, 4/4, 041005.
- [10] KAPJOR A., SMATANOVA H., HUZVAR J., GRESSAK T., JANDACKA J., 2013, *Optimization of Heat Transfer Oriented Surfaces by Thermovision and Using CFD Method*, Structure and Environment, 5/4, 41–44.
- [11] KALACZYNSKI T., LUKASIEWICZ M., MUSIAL J., LISS M., KASPROWICZ T.B., 2020, *Analysis of the Diagnostic Potential Thermovision Research in the Technical Condition Assessment of Spark Ignition Engines Injectors*, Engineering Mechanics, 26, 262–265.
- [12] PIECUCH G., MADERA M., ZABINSKI T., 2019, *Diagnostics of Welding Process Based on Thermovision Images Using Convolutional Neural Network*, IOP Conference Series: Materials Science and Engineering, 710/1.
- [13] WANG R., ZHAN X., BAI H., DONG E., CHENG Z., JIA X., 2022, *A Review of Fault Diagnosis Methods for Rotating Machinery Using Infrared Thermography*, Micromachines, 13, 1644.
- [14] MEZYK J., 2015, *Monitoring Material Joining Processes with use of Advanced Vision Methods*, Maintenance Problems, 1/96, 37–46.
- [15] SWIC A., WOLOS D., ZUBRZYCKI J., OPIELAK M., GOLA A., TARANENKO V., 2014, *Accuracy Control in the Machining of Low Rigidity Shafts*, Applied Mechanics and Materials, 613, 357–367.
- [16] BYRNE G., DORNFELD D., DENKENA B., 2003, *Advancing Cutting Technology*, CIRP Annals, 52/2, 483–507.
- [17] SENTHILKUMAR N., GANAPATHY T., TAMIZHARASAN T., 2014, *Optimisation of Machining and Geometrical Parameters in Turning Process Using Taguchi Method*, Australian Journal of Mechanical Engineering, 12/2, 233–246.
- [18] BEMBENEK M., KUDELSKI R., PAWLIK J., KOWALSKI Ł., 2021, *The Influence of CNC Turning with VBMT, RCMX, 3ER, and MGMN Type Indexable Inserts on West African Ebony/Diospyros Crassiflora, San Domingo Boxwood/Phyllostylon Brasiliense, Rio Rosewood/Dalbergia Nigra, Beechwood/Fagus Sylvatica, Oakwood/Quercus Robur, and Pinewood/Pinus Silvestris Surface Roughness*, Materials, 14, 5625.
- [19] PANWAR V., SHARMA D.K., PRADEEP K.V., JAIN A., THAKAR Ch., 2021, *Experimental Investigations and Optimization of Surface Roughness in Turning of EN 36 alloy steel using response surface methodology and genetic algorithm*, Materials today: proceedings, 46, 6474–6481.

- [20] DOAN T.K., NGUYEN T.T., VAN. A.L., 2023, *Multi-Objective Optimization of the Rotary Turning of Hardened Mold Steel for Energy Saving and Surface Roughness Improvements*, Journal of Machine Engineering, 23/4, 101–121, <https://doi.org/10.36897/jme/172877>.
- [21] QEHAJA N., JAKUPI K., BUNJAKU A., BRUČI M., OSMANI H., 2015, *Effect of Machining Parameters and Machining Time on Surface Roughness in Dry Turning Process*, Procedia Engineering, 100, 135–140.
- [22] ZHAO G.Y., LIU Z.Y., HE Y., CAO H.J., GUO Y.B., 2017, *Energy Consumption in Machining: Classification, Prediction, and Reduction Strategy*, Energy, 133, 142–157.
- [23] SHROUF F., ORDIERES-MERE J., GARCIA-SANCHEZ A., ORTEGA-MIER M., 2014, *Optimizing the Production Scheduling of a Single Machine to Minimize Total Energy Consumption Costs*, Journal of Cleaner Production, 67, 197–207.
- [24] GRZESIK W., 2020, *Modelling of Heat Generation and Transfer in Metal Cutting: a Short Review*, Journal of Machine Engineering, 20/1, 24–33, <https://doi.org/10.36897/jme/117814>.
- [25] NIEŚŁONY P., GRZESIK W., LASKOWSKI P., ZAK K., 2015, *Numerical 3D Simulation and Experimental Analysis of Tribological Aspects in Turning Inconel 718 alloy*, Journal of Machine Engineering, 15/1, 47–57.
- [26] SHEROV K., MUSSAYEV M., USSERBAYEV M., MAGAVIN S., ABISHEVA N., KARSAKOVA N., MYRZAKHMET B., 2022, *Investigation of the Method of Thermal Friction Turn-Milling of High Strength Materials*, Journal of Applied Engineering Science, 20/1, 13–18.
- [27] TATSIY R.M., PAZEN O.Y., VOVK S.Y., ROPYAK L.Y., PRYHOROVSKA T.O., 2019, *Numerical Study on Heat Transfer in Multilayered Structures of Main Geometric Forms Made of Different Materials*, Journal of the Serbian Society for Computational Mechanics, 13/2, 36–55.
- [28] GRZESIK W., RECH J., ZAK K., CLAUDIN C., *Machining Performance of Pearlitic–Ferritic Nodular Cast Iron with Coated Carbide and Silicon Nitride Ceramic Tools*, International Journal of Machine Tools and Manufacture, 49/2, 125–133.
- [29] JAFARIAN F., CIARAN M.I., UMBRELLO D., ARRAZOLA P.J., FILICE L., AMIRABADI H., 2014, *Finite Element Simulation of Machining Inconel 718 Alloy Including Microstructure Changes*, International Journal of Mechanical Sciences, 88, 110–121.
- [30] WANG F., ZHAO J., LI A., ZHANG H., 2014, *Effects of Cutting Conditions on Microhardness and Microstructure in High-Speed Milling of H13 Tool Steel*, The International Journal of Advanced Manufacturing Technology, 73, 137–146.
- [31] BEMBENEK M., KOPEI V., ROPYAK L., LEVCHUK K., 2023, *Stressed State of Chrome Parts During Diamond Burnishing*, Metal. & Advanc. Techn., 45/2, 239–250, <https://doi.org/10.15407/mfint.45.02.0239>.
- [32] MARUDA R.W., KROLCZYK G.M., MICHALSKI M., 2017, *Structural and Microhardness Changes After Turning of the AISI 1045 Steel for Minimum Quantity Cooling Lubrication*, Journal of Materials Engineering and Performance, 26, 431–438.
- [33] ROTELLA G., DILLON O.W., UMBRELLO D., SETTINERI L., JAWAHIR I.S., 2014, *The Effects of Cooling Conditions on Surface Integrity in Machining of Ti6Al4V Alloy*, The International Journal of Advanced Manufacturing Technology, 71, 47–55.
- [34] YANG Y., JIN L., ZHU J., 2020, *Study on Cutting Force, Cutting Temperature and Machining Residual Stress in Precision Turning of Pure Iron with Different Grain Sizes*, Chinese J. of Mechanical Engineering, 33/53, 1–9.
- [35] ZHAO G.Y., LIU Z.Y., HE Y., CAO H.J., GUO Y.B., 2017, *Energy Consumption in Machining: Classification, Prediction, and Reduction Strategy*, Energy, 133, 142–157.
- [36] AKHIL C., ANANTHAVISHNU M., AKHIL C., AFEEZ P., AKHILESH R., RAJAN R., 2016, *Measurement of Cutting Temperature During Machining*, Journal of Mechanical and Civil Engineering, 13/2, 108–122.
- [37] STRUZIKIEWICZ G., 2013, *Analysis of Temperature Measurement Correctness in Cutting Zone During 4H13 Steel Turning*, Inżynieria Maszyn, 18/4, 72–85, (in Polish).
- [38] BRILI N., FICKO M., KLANCNIK S., 2021, *Automatic Identification of Tool Wear Based on Thermography and a Convolutional Neural Network During the Turning Process*, Sensors, 21/5, 1917, <https://doi.org/10.3390/s21051917>.
- [39] KISZKA P., GRZESIK W., RECH J., 2015, *Analysis of Temperature Distribution Layout Within the Cutting Zone by Means of an Infrared Camera*, Mechanik, 3, 197–200.
- [40] BORUI: EN-GJL-250 specification, <https://www.iron-foundry.com/en-gjl-250-cast-iron-gg25.html> (available on-line on 26-06-2023).
- [41] BASEDOSTEEL: 1.4301 specification, <https://www.basedosteel.com/en/materials/material/14301.html> (available on-line at 26-06-2023).
- [42] GRZESIK W., 1998, *Basics of Materials Cutting*, WNT, Warszawa.
- [43] SANDVIK: <https://www.sandvik.coromant.com/pl-pl/knowledge/materials/workpiece-materials?Country=pl>,
- [44] PALOPOSKI T., LIEDQUIST L., 2005, *Steel Emissivity at High Temperatures*, Espoo, Publisher VTT Technical Research Centre of Finland.